# Model simplification and validation of virtual prototypes for vehicular antenna design

Yousaf, Irfan Mehmood; Katare, Kranti Kumar; Lau, Buon Kiong

*Published in:*
14th European Conference on Antennas and Propagation, EuCAP 2020

*DOI:*
10.23919/EuCAP48036.2020.9136070

2020

*Document Version:*
Peer reviewed version (aka post-print)

# Model Simplification and Validation of Virtual Prototypes for Vehicular Antenna Design

Irfan Mehmood Yousaf[1,2], Kranti Kumar Katare[1,2], Buon Kiong Lau[2]
[1] Volvo Car Corporation, Gothenburg, Sweden, irfan.yousaf@volvocars.com
[2] Department of Electrical and Information Technology, Lund University, Lund, Sweden

***Abstract*—Wireless connectivity is becoming an important feature in cars, which together with recent developments in car design point to the need to accurately predict the performance of real antennas in simulation, to speed up the design cycle. However, it is challenging to accurately represent structurally complex real cars in simulation. This paper proposes a car model simplification approach for designing vehicular antennas, exemplified using three progressively simplified models of a hatchback car. For validation, a monopole and a PIFA operating at 800 MHz and 2.4 GHz, respectively, were mounted and simulated at two locations on these prototypes. The proposed scheme reduced the computational time to less than a third, while maintaining similar simulated antenna performance. Specifically, the antenna patterns of the simplest prototype and original one are correlated by 84% and 59% at 800 MHz and 2.4 GHz, respectively. Therefore, the proposed scheme is promising for real application.**

***Index Terms*—Vehicular antenna, model simplification, monopole antenna, PIFA, computational time.**

## I. INTRODUCTION

Nowadays, cars are perceived to be much more than a way to transport people from one place to another place. The focus is on improving the experience of the passengers during the journey. This emphasis will become even more important when autonomous cars are finally deployed, since the traditional drivers will now have the freedom to do other things. This opens up a lot of possibilities for different services that can be offered, and wireless connectivity is crucial for enabling many of these services [1].

Furthermore, car design is also evolving to match the future needs of the passengers. The environment inside the car becomes important because people who spend a lot of time inside the small interior while traveling long distances are demanding for better comfort and the feel of open space. Glass is already used in the upper part of many cars to let the natural light through and provide a better view of the surroundings [2]. This trend has negatively affected antenna placement on cars and posed new challenges for designing car antennas. The ground plane for the roof antennas is disappearing as the roof is increasingly made of glass. Also, the desire to hide antennas from view (as was the trend for mobile terminal antennas around 20 years ago) means that their locations are more restricted, which can degrade their performance. Moreover, many more antennas are now needed to support different services as well as to enable higher throughput [3]. As a result, better integration of car antennas is crucial, which in general requires the surroundings (the entire car platform) to be accounted for.

In particular, a car has many electronic control units (ECUs) and cables connecting them. There are also many other parts in the car that can significantly affect antenna performance, such as seats, dashboard and trim panels. The antennas are normally not more than a few centimeters in size, which are dwarfed by the size of the cars (e.g., 4 to 6 meters). Hence, running an antenna simulation that includes the whole environment becomes very challenging because of the complex surroundings of the antenna and the electrically large car for the frequencies used in common applications. Therefore, there is a need to develop simplified models of the car to be able to find a good compromise between the accuracy of the simulation results and the size/complexity of the simulation problem. For industrial antenna design relying on optimization over multiple iterations, there should be enough information in the simplified model to provide "good enough" prediction of the antenna performance in each iteration within a reasonable time [4].

Simplification of car models for vehicular antenna design is a relatively uncharted topic in the literature. Specifically, existing work focuses on the use of simple car models to study the effect of the car body on antenna performance [5], [6], the effect of car seats and dashboard on the electromagnetic environment inside the car [7], and the effect of material properties of different interior parts on the in-car channel [8], [9]. However, these simple car structures only consist of simple flat surfaces, which are not representative of modern cars. Moreover, no attempt is made to study the effect of model simplification on antenna performance.

Based on a more realistic car model, accounting for the curvatures of a modern car body (of Volvo XC60) but retaining only the main part of the metallic frame, a simulation framework for studying the impact of electromagnetic interference on vehicular antenna performance is proposed in [10]. In addition, a similar car model as [10] (but with the inclusion of glass windows) was used to investigate the influence of RF cables on in-vehicle channel measurements [11]. But as in earlier studies [5]-[9], [10] and [11] do not explore the relationship between the simplification of car body and the accuracy of simulated antenna performance.

Therefore, the main aim of this work is to propose a model simplification approach that can facilitate shorter computational time, while retaining similar simulated performance of vehicular antennas. To validate the applicability of the proposed scheme, two different antenna structures are considered, i.e., monopole and planar inverted-F antenna (PIFA), with omni and directional patterns intended for LTE and WLAN applications at 800 MHz and 2.4 GHz bands, respectively. The two antennas are mounted on two different locations of the car (rooftop and just under the roof). Three prototypes (Models A, B and C) of a hatchback car, representing different levels of structural complexity, are used to demonstrate the model simplification approach. It will be shown that significant simplifications can be performed on the car model while preserving the accuracy of the simulated antenna performance of the most complex model (Model A).

To the author's knowledge, this systematic study is the first of its kind and it can provide a roadmap for efficient design of integrated vehicular antennas with good accuracy despite significantly reduced simulation time/complexity. Such a design framework is a powerful enabler for virtual prototyping of future cars.

## II. Simplifications of Car Model

For small cars, the data file of a professional CAD tool (e.g., CATIA by Dassault Systems) that contains the complete geometrical model of a car is normally around 50 GB in size. CATIA is a popular tool in the automotive industry for the detailed designing and physical packaging of the complete car, including all the electrical and mechanical components. The detailed model is needed for tool design, tolerance calculations and assembly simulations. Bringing this massive amount information into a commercial full-wave simulation tool for antenna design is not feasible even for powerful computers available to antenna designers in the car industry. The required number of meshes and the resulting problem are too large to be handled efficiently. Therefore, a systematic approach of simplifying the car model by actively retaining or removing interior parts of a complete hatchback car model is presented in this section.

The basic idea for the simplification procedure is to establish a trade-off between the performance and the computational time of vehicular antenna simulation during the antenna design phrase. To demonstrate the proposed scheme, three virtual prototypes (Models A, B and C) of Volvo S60, a hatchback car, were formed (see Fig. 1). All the parts, which were deemed by their sizes and electrical properties to have only a minor influence on the electro-magnetic environment, were left out of the prototypes. A preliminary step was taken to exclude parts that are made of plastic, wood, foam, rubber and other non-metallic materials. Hence, all the car prototypes considered here consist of the metallic car body and metallic parts. Although the removal of non-metallic parts from the car body reduced the problem size to one third of the original size, the computational time was still very long.

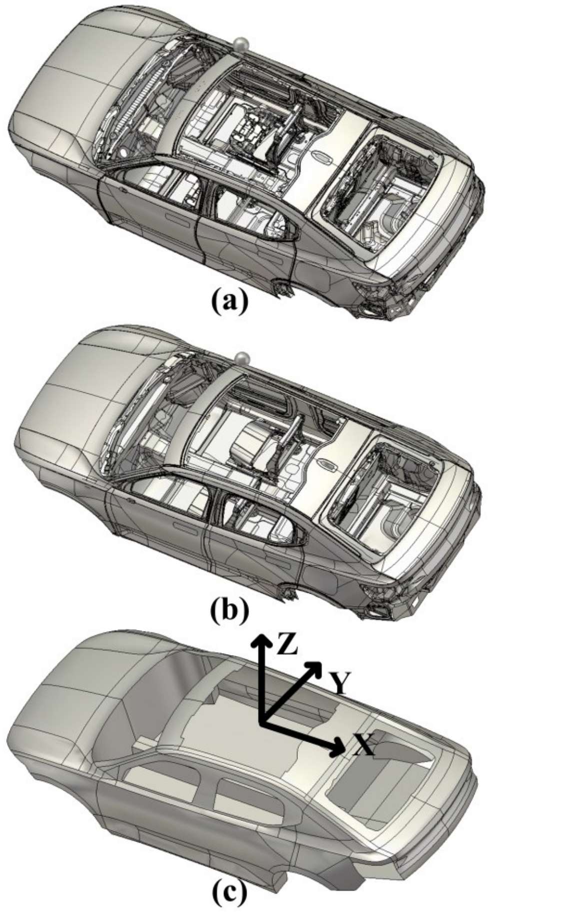


Fig. 1. Three virtual prototypes of the hatchback car, with increasing degree of model simplifications: (a) Model A, (b) Model B, (c) Model C.

Therefore, a novel approach is proposed in this work: First, all the car body parts that are shielded from the radiation of antennas placed inside or on the exterior of the car, such as the parts in the engine bay and at the bottom of the car, are excluded from the simplified model. Secondly, many metal parts that are very small in size (small plates, nuts, bolts and multiple layers of metals) are expected to only have limited impact on the antenna performance. Therefore, to reduce the computation time, these small metallic parts can be ignored during the simulation process. For further simplification, the remaining metallic parts of the car body can be replaced with thin metal sheets.

Based on the above discussion, three virtual prototypes (Models A, B and C) were created. Model A is a fully metallic car body (see Fig. 1(a)), which was obtained after removing all non-metallic parts as well as shielded metallic parts. This prototype was further simplified to Model B by removing small metallic parts from inside of the car, as depicted in Fig. 1(b). Finally, the most simplified version (Model C, as shown in Fig. 1(c)) was prepared, where a lot of geometrical information of both the inner and outer parts of the car body was removed. In this version, the dashboard and the floor of the car were replaced with straight metallic sheets. Moreover, the metallic seat frames and other larger metallic structures were also removed.

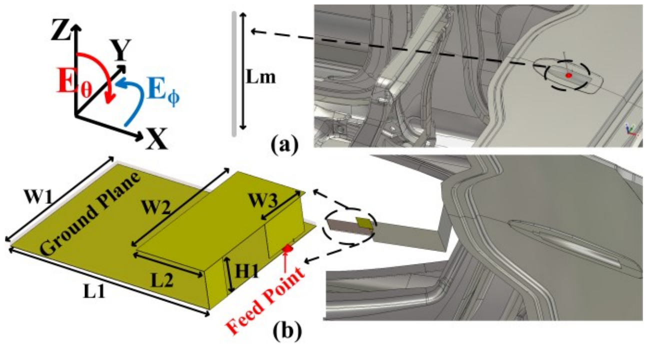


Fig. 2. Antennas and their locations on the hatchback car. (a) Monopole antenna (Lm = 75, wire diameter = 4), (b) PIFA (L1 = 57.50, W1 = 39.2, L2 = 19.4, W2 = 37.1, H1 = 9.1, W3 = 13) (all lengths are in mm).

## III. Antenna Design And Placement

Two different antenna configurations were integrated with the three car models. The first antenna is a standard quarter-wave monopole with omnidirectional pattern in the upper hemisphere when integrated on the car roof. It was designed for cellular (LTE) application at 800 MHz. It was intentionally placed at the location of the common "shark fin" roof antenna (see Fig. 2(a)). Typically, the shark fin antenna consists of multiple monopole antennas for multi-band and multiple-input multiple-output (MIMO) operations.

To investigate the potential of the model simplification approach more thoroughly, the second antenna was chosen to be a PIFA, which has a directional (broadside) radiation pattern. It is designed with the center frequency of 2.4 GHz for WLAN (or WiFi) application. The operating frequency was chosen to be three times larger than that of the monopole, to present a more challenging case for antenna simulation, due to the larger electrical size of the structure requiring significantly more mesh cells and computational efforts. The antenna is attached to a small ground plane slightly below the sun roof, as shown in Fig. 2(b). The chosen antenna location facilitates a hidden antenna solution, and it also enables both in-car and infrastructure WLAN coverage. For example, the car may need to be connected to the workshop computer system for remote diagnostic and firmware/software updates. As will be discussed in Section IV, the location under the rooftop also provides a different environment for the antenna, as antenna radiation from this location tends to interact with the car interior (i.e., a cavity with openings) more than that from the rooftop location, as the roof shields most of the radiation from the interior.

## IV. Simulation Results And Discussions

The antenna configurations given in the previous section were simulated with the car models provided in Section II. The time-domain solver of 2018 CST Microwave Studio was used for the full-wave simulations. The CST time-domain solver is based on the finite integration technique (FIT) [12]. For convenience, and with no loss in generality, all metallic parts were modeled as perfect electric conductor (PEC), giving 100% radiation efficiency.

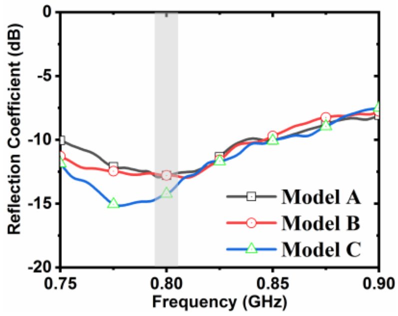


Fig. 3. Reflection coefficients of the monopole antenna mounted on three different virtual prototypes of the hatchback car.

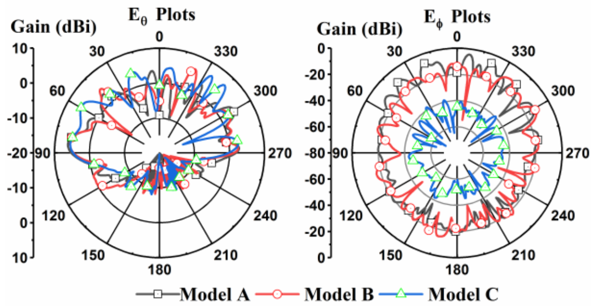


Fig. 4. Radiation patterns of monopole antenna (at 800 MHz) with three different models of the hatchback car in the XZ-Plane.

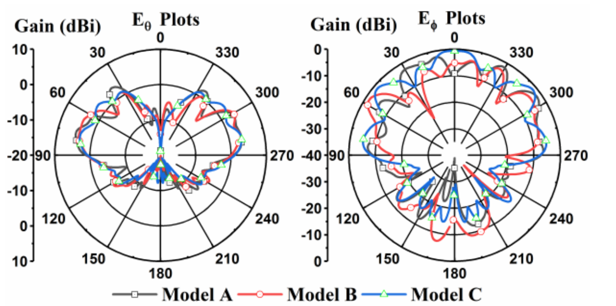


Fig. 5. Radiation patterns of monopole antenna (at 800 MHz) with three different models of the hatchback car in the YZ-Plane.

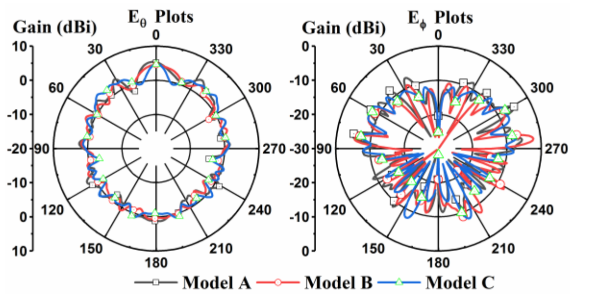


Fig. 6. Radiation patterns of monopole antenna (at 800 MHz) with three different models of the hatchback car in the XY-Plane.

### *A. Monopole Antenna Performance with Car Models*

The reflection coefficients of the monopole antenna (see Fig. 3) are almost the same when mounted on Models A, B and C. This is due to nearfield environment (e.g., the ground plane in the vicinity of the monopole) being nearly the same.

The radiation patterns of this antenna in the XZ-, YZ- and XY-planes are shown in Fig. 4 to Fig. 6, respectively. $E_\theta$ and $E_\phi$ represent the co- and cross-polar (electric field) components of the farfield radiation pattern. From Fig. 4, it can be observed that the co-polar ($E_\theta$) pattern of monopole is slightly directional towards the back side of the car. This is due to the roof (below the monopole) slightly tilting downwards towards the back side of the car. Apart from this, since antenna is placed symmetrically in the YZ-plane (see Fig. 2(a)), almost symmetrical co-polar ($E_\theta$) patterns are obtained in the same YZ-plane (see Fig. 5). The cross-polar component of electric field ($E_\phi$) is seen to be generally below -10 dBi in both XZ- (Fig. 4) and XY-planes (see Fig. 6), but significantly increasing to 0 dB in the YZ-plane (see Fig. 5). The very low cross-polar component in the XZ plane (mostly below -40 dBi) for Model C is likely an artefact of the time-domain solver, since this behavior cannot be reproduced in other full-wave solvers (e.g., CST frequency domain solver).

Comparing between the results for Models A, B and C, the radiation patterns for Models A and B are more similar to each other than to Model C, especially in the dominant $E_\theta$ component. This observation is confirmed by Table I, which shows the magnitude of the complex correlation coefficient between the radiation patterns. This result can be due to large metal parts in Models A and B (e.g., car seats and dashboard) being removed in Model C. Hence, even though the car roof partially shields the monopole radiation from "seeing" the car interior, major changes in the car interior are still reflected in the radiation pattern. In addition, Table I also shows that despite significant simplifications in the car models, very high correlation of 0.84 is still obtained in the worst case, indicating that for this application, the proposed model simplification approach is feasible from the viewpoint of maintaining the antenna performance.

TABLE I. CORRELATION COEFFICIENTS OF ANTENNA PATTERNS BETWEEN DIFFERENT PROTOTYPES AT CENTER FREQUENCY $f_0$

| Models | Monopole antenna ($f_0$ = 800 MHz) | PIFA antenna ($f_0$ = 2.4 GHz) |
|---|---|---|
| Model A and B | 0.91 | 0.73 |
| Model A and C | 0.84 | 0.59 |

### B. *PIFA Performance with Car Models*

The reflection coefficients of the PIFA when mounted on Models A, B and C are shown in Fig. 7. The matching slightly worsens with the simpler models, but very good matching (i.e., below -10 dB) is still retained within the band of interest (2.4-2.5 GHz).

The corresponding PIFA radiation patterns for these three car models in the XZ-plane (E-Plane) and YZ-plane (H-Plane) are shown in Figs. 8 and 9, respectively. It can be seen that the $E_\phi$ component is significantly higher in the YZ-plane than in the XZ plane, but this is similar to the behavior of a stand-alone PIFA, when placed in the center of a large ground plane (e.g., 1 m × 1 m). Hence, it may not reflect the effect of the car body. In addition, the large fluctuations in the antenna gain across the elevation angles, which are not present in a standalone PIFA, are attributed to the reflections from the interior of the car body.

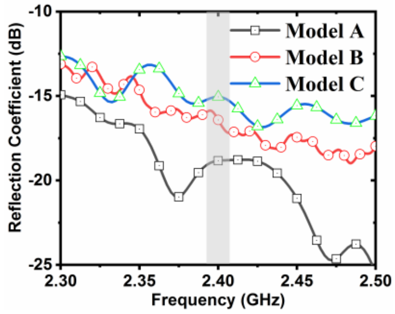


Fig. 7. Reflection coefficient of the PIFA mounted in three different virtual prototypes of the hatchback car.

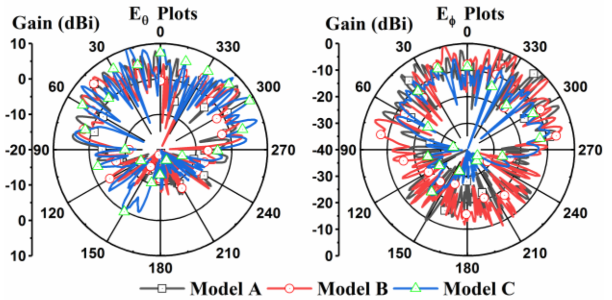


Fig. 8. Radiation patterns of PIFA (at 2.4 GHz) with three different virtual prototypes of the hatchback car in the XZ-Plane.

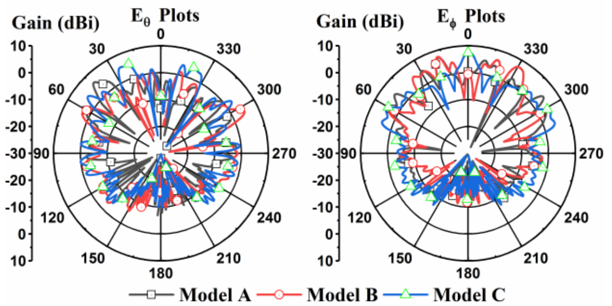


Fig. 9. Radiation patterns of PIFA (at the frequency of 2.4 GHz) with three different virtual prototypes of the hatchback car in the YZ-Plane.

The rapid fluctuations in the antenna gain complicate visual comparison of the radiation patterns of the PIFA for Models A, B, and C. However, as can be seen in Table I, the patterns are still correlated to some degree between the different models, i.e., by almost 0.6 even between Model A and the simplest model (Model C). Furthermore, it should be noted that for Model C, the seat frames and the dashboard were removed, which result in a very different electro-magnetic environment inside the car. It has been shown in [11] that even minor variations of the metallic parts can result in different distribution of electric fields and currents inside the car. However, further work is necessary to determine an appropriate cutoff point for pattern similarity for the purpose of vehicular antenna simulation.

Overall, the analysis on the effect of model simplification on the simulated antenna performance indicates that, under certain conditions, simplification results in limited impact. In particular, if the antenna is located on the exterior of the car, the pattern is shielded from major changes in the interior.

### C. Computational Time and Complexity of Simulation

For the model simplification scheme described in Section II to be worthwhile, it must offer significant savings to computational time and effort. The simulation server used in this study has the following specifications: Intel Xeon CPU (E5-2620 2 GHz Dual Processor), 192 GB RAM and two GPUs (Nvidia Quadro M600 12GB with 3072 GPU cores). Tables II and III list the number of mesh cells and time needed to simulate the monopole and PIFA performance, respectively, on each of the three models. All the simulations (on CST time-domain solver) are set to end when the convergence accuracy reaches -40 dB (i.e., they are not limited by the number of simulation cycles). As can be seen in the two tables, the computational time scales almost linearly with the number of mesh cells for each antenna type, as is expected from FIT and time-domain techniques [13]. The computational time is significantly larger for the PIFA cases than the monopole cases, and this explained by its higher operating frequency, which requires a smaller mesh size, and in turn leads to a smaller time step (by the Courant stability condition) to simulate the propagation of electromagnetic field in the computational volume [13]. In addition, the large memory of 192 GB also means that physical memory size is not expected to be a limiting factor, and this is confirmed by inspecting the available memory on the server during simulation runs.

TABLE II. SIMULATION COMPLEXITY/TIME FOR MONOPOLE

| Monopole | No. of mesh cells | Computational time (hours) |
|---|---|---|
| Model A | 35 205 720 | 1.7 |
| Model B | 18 827 136 | 0.9 |
| Model C | 13 715 520 | 0.5 |

TABLE III. SIMULATION COMPLEXITY/TIME FOR PIFA

| PIFA | No. of mesh cells | Computational time (hours) |
|---|---|---|
| Model A | 193 872 640 | 68 |
| Model B | 110 085 000 | 38 |
| Model C | 55 012 068 | 17.2 |

The two tables show that model simplification from Models A to B almost halves the required number of mesh cells and simulation time, and depending on the antenna, further savings of roughly 40-50% are achieved. If Model C can be used (according to the required accuracy in antenna performance), then the simplification scheme reduces the simulation time to less than one third, not including the initial simplifications (to reach Model A) in removing non-metallic parts and other metallic parts (e.g., car engine) shielded by the metal shell of the interior.

## V. CONCLUSIONS

A systematic study on the simplification of car models for vehicular antenna simulation is presented in this work. A time-domain solver is used for the full-wave simulations. The results show good potential for the proposed model simplification scheme to achieve up to 70% reduction of simulation time/complexity while retaining good accuracy (i.e., 0.84 correlation in the radiation patterns). Moreover, significant cross-polar component was observed in the YZ-plane for both antennas. This can be due to reflections and diffractions on the car body, and it can be an interesting aspect for further study. Finally, it should be noted that this study focuses on the loss of accuracy of the simulated antenna performance due to simplifications. Validation of the simulated results against measured results based on equivalent prototype antennas on a real car is a subject for future work.

ACKNOWLEDGMENT

This work is supported in part by the VINNOVA FFI Programme under Grant no. 2014-01403 and in part by the Swedish Research Council under Grant no. 2010-468.

REFERENCES

[1] A. Meola, “Automotive industry trends: IoT connected smart cars and vehicles,” 2016. [Online]. Available: http://www.businessinsider .com/internet-of-things-connected-smart-cars-2016-10 [Accessed: Oct. 20, 2017]

[2] M. B. Diez, W. Pascher, and S. Lindenmeier, “Electromagnetic characterization of automotive sunroofs for car-to-X applications,” in *46th European Microwave Conference (EuMC)*, London, UK, Oct. 4-6, 2016, pp. 1323-1326.

[3] O. Kwon, R. Song, and B. Kim, "A fully integrated shark-fin antenna for MIMO-LTE, GPS, WLAN, and WAVE applications,” *IEEE Antennas Wireless Propag. Lett.*, vol. 17, no. 4, pp. 600-603, 2018.

[4] A. Nogueira de Sao Jose, et al., “Computational savings based on Three-Dimensional automotive geometries’ simplifications in electro-magnetics simulations,” in *Proc. 2013 SBMO/IEEE MTT-S Int. Microw. Optoelectron. Conf. (IMOC),* Rio de Janeiro, Brazil, Aug. 4-7, 2013, pp. 1-5.

[5] K. Taguchi, S. Imai, ,T. Kashiwa, H. Kuribayashi, and S. Komatsu, “Distance dependence of electric field pattern for an antenna mounted on a car in UHF band,” *Microw. Opt. Technol. Lett.*, vol. 55, pp. 2182-2186, 2013.

[6] S. Imai, K. Taguchi, T. Kashiwa, and T. Kawamura, “Effects of car body on radiation pattern of car antenna mounted on side mirror for inter-vehicle communications,” in *Proc. IEEE Antennas Propag. Soc. Int. Symp. (APSURSI)*, Memphis, TN, Jul. 6-11, 2014, pp. 601-602.

[7] A. R. Ruddle, “Influence of dielectric materials on invehicle electromagnetic fields,” in *Proc. IET Seminar Electromagn. Propag. Structures Buildings*, London, UK, Dec. 4, 2008, pp. 1-6.

[8] A. R. Ruddle, H. Zhang, L. Low, J. Rigelsford, and R. J. Langley, “Numerical investigation of the impact of dielectric components on electromagnetic field distributions in the passenger compartment of a vehicle,” in Proc. *20th Int. Zurich Symp. Electromagn. Compat.,* Zurich, Jan. 12-16, 2009, pp. 213-216.

[9] A. Schoof, T. Stadtler, and J. L. T. Haseborg, “Simulation and measurement of the propagation of Bluetooth signals in automobiles,” in *Proc. IEEE Int. Symp. Electromagn. Compat.,* Istanbul, Turkey, May 11-16, 2003, pp. 1297-1300.

[10] I. M. Yousaf, B. K. Lau, and B. Bergqvist, “Simulation of internal electromagnetic interference for vehicular antenna performance evaluation,” in *Proc. 10th Europ. Conf. Antennas Propag. (EuCAP)*, Davos, Switzerland, Apr. 10-15, 2016.

[11] I. M. Yousaf and B. K. Lau, “Impact of RF cables on the electromagnetic environment in vehicles,” in *Proc. IEEE Int. Symp. Personal, Indoor, Mobile Radio Commun.*, Montreal, Canada, Oct. 8-13, 2017.

[12] T. Weiland, “A discretization method for the solution of Maxwell's equations for six-component fields,” *Archiv für Elektronik und Uebertragungstechnik (AEÜ)* [*Electron. Commun.*], vol. 31, pp. 116-120, Mar. 1977.

[13] CST, “Understanding time domain meshing in CST Microwave Studio®” White Paper, Jul. 2010.